EUROPEAN ORGANIZATION FOR NUCLEAR RESEARCH

CERN/EP 86-164
21 October 1986

EVIDENCE FOR HIGHER TWIST MECHANISMS IN PROMPT ρ^0-MESON PRODUCTION AT $p_T > 2$ GeV/c IN 300 GeV/c π^-N INTERACTIONS

Athens[1]-Bari[2]-Birmingham[3]-CERN[4]-Paris (Collège de France)[5]-
Paris (LPNHE)[6] Collaboration

M. Benayoun[5], W. Beusch[4], I.J. Bloodworth[3], A.J. Burns[4], J.N. Carney[3], B.R. French[4], B. Ghidini[2], Y. Goldschmidt-Clermont[4], G. Ingelman[4(*)], A. Jacholkowski[6], J. Kahane[5], J.B. Kinson[3], K. Knudson[4], J.C. Lassalle[4], V. Lenti[2], Ph. Leruste[5], A. Malamant[5], J.L. Narjoux[5], F. Navach[2], C. Néaume[6], A. Palano[2], R. Petronzio[4], M. Pimenta[4(**)], I.C. Print[3], E. Quercigh[4], M. Sené[6], R. Sené[5], H.R. Shaylor[3], M. Stassinaki[1], Z. Strachman[6], M.T. Trainor[3], G. Vassiliadis[1], O. Villalobos Baillie[3], M.F. Votruba[3], G. Zito[2] and R. Zitoun[6]

ABSTRACT

The production of ρ^0 mesons in hadronic interactions is investigated at high transverse momentum ($p_T > 2$ GeV/c). The data come from a sample of π^-N interactions at 300 GeV/c obtained at the CERN OMEGA spectrometer, requiring a $\rho^0 \to \pi^+\pi^-$ with p_T(pair) > 2 GeV/c to recoil against an opposite particle with p_T (opposite) > 1 GeV/c. The signal/(signal + background) ratio of ρ^0 production shows an increase of 38% as $x_E = p_T(\text{opposite})/p_T(\text{pair})$ decreases from $0.5 < x_E < 1$ to $x_E \leq 0.5$. This increase is not compatible with a QCD model of parton scattering and subsequent fragmentation. It is interpreted as evidence for direct ρ^0 production via QCD higher twist processes, in terms of which a quantitative agreement with the data is found.

Submitted to Physics Letters B

(*) Now at DESY, Hamburg.
(**) Now at CFMG-INIC, Lisbon, Portugal.

EP/3220P/EQ/em

In the framework of Quantum Chromo Dynamics (QCD), high p_T particles are mainly produced "indirectly" via parton scattering and fragmentation (fig. 1(a)). "Direct" meson production, via a higher twist mechanism such as fig. 1(b), is also predicted to exist and to be detectable at high p_T [1,2]. Such direct processes have not yet been isolated experimentally, although experimental evidence for and against higher twist effects has been presented in other contexts [3].

This paper investigates the mechanism of ρ^o production at high p_T (> 2 GeV/c) in π^-N interactions at 300 GeV/c. In particular, in comparing the experimental results with the predictions of QCD-based models it is found necessary to include direct production of ρ^o via higher twist processes in order to explain the observations.

We note that in the direct process (fig. 1(b)) the ρ^o picks up the full momentum transfer carried by the exchange, while in the indirect process (fig. 1(a)) the ρ^o shares the momentum transfer with the other fragmentation products. This feature is exploited in a multiparticle trigger, which isolates events in which a high p_T ρ^o meson recoils against one high p_T particle. The trigger selects events with three particles having p_T > .9 GeV/c and c.m.s. rapidities $-1 < Y^{CM} < 1$, i.e. a pair of oppositely charged particles produced opposite in azimuth to a third one (fig. 1(c)).

A 300 GeV/c π^- beam interacts in a 4.8 cm Be target in the CERN OMEGA Spectrometer [4]. The charged tracks are detected by 15 multiwire proportional chambers (MWPCs) in a magnetic field with a bending power of 5.8 Tm and two drift chambers (DC1, DC2) (fig. 2(a)). Two downstream multicell Cerenkov counters (C_1, C_2) allow for a separation between π and K mesons between 4 and 17.8 GeV/c.

The trigger electronics using the MBNIM system [5] allows for measurements of the transverse momentum p_T of several particles. It uses two hodoscopes (HZ1, HZ2) and two MWPC's with two planes each (MY1, MY2 and MY3, MY4) specifically designed for the detection of high p_T particles. The hodoscopes have four quadrants, each made of 15 horizontal slabs. The sensitive region of the hodoscopes has a "butterfly" shape (fig. 2(b)) which lies outside the reach of particles with p_T < 0.6 GeV/c.

The slabs of HZ1 and HZ2 subtend the same solid angle for particles leaving the vertex. A pair of correlated hits in HZ1 and HZ2 gives a measurement of the dip angle λ. The MY planes have 4 mm pitch vertical wires. Graphite paint on the cathodes defines three electrically insulated regions, with butterfly shapes matching the outlines of the hodoscopes HZ1 and HZ2. The voltages are adjusted so that the pair MY1, MY3 records particles only in the upper part, and MY2, MY4 only in the lower part. Two hits in the MY's (e.g. MY1 and MY3) measure the horizontal component of the production angle and the radius of curvature. From these data and from the dip angle λ, the MBNIM system computes the transverse momenta p_T in ~ 30 μs with an accuracy of ~ 10%.

An incident intensity of 10^7 π^- per pulse and a trigger rate of ~ 80 events per burst led to about 7 million triggers being recorded in a 12-day run (integrated luminosity 2000 nb^{-1}). The events were reconstructed by the TRIDENT program [6]. The pattern recognition uses the higher precision of the drift chambers to define track segments, which were followed upstream to the 15 MWPCs and target. The reconstruction of angles and momenta gives a resolution in effective mass of ± 15 MeV for pairs of high p_T tracks.

The data presented here are based on a sample of 266611 reconstructed events which satisfy the following requirements:

(a) 3 and only 3 trigger tracks from the primary vertex, each with p_T >1 GeV/c.

(b) A pair of these tracks, of opposite charges, opposite in azimuth to the third track. (1)

(c) $p_T(\text{pair}) > 2$ GeV/c.

(d) $-0.45 < Y^{CM}_{pair} < 0.45$.

The invariant mass spectrum for the pairs of high p_T particles assuming both particles in the pair to be pions, is shown in fig. 3(a). Clear signals are present in the $\rho^0(770)$ and $f^0(1270)$ mass regions.

A fit of the $\pi^+\pi^-$ mass spectrum by the method described below, yields 13074 ± 400 ρ^0. From this number, a cross section for ρ^0 production for

$p_T(\rho^o) > 2$ GeV/c, $-.45 < Y^{CM}_{\rho^o} < .45$ and p_T (opposite) > 1 GeV/c is determined. Taking into account the measured detection efficiencies of the trigger and associated electronics, the efficiency of the spectrometer and of the TRIDENT reconstruction, the geometrical acceptance of the apparatus and assuming an isotropic angular decay distribution for the ρ^o, we find $\sigma(\rho^o) = 0.89 \pm 0.3$ μb(*) where the error contains both the statistical and systematic effects.

For each event we compute the quantity

$$x_E = \frac{p_T(\text{opposite})}{p_T(\text{pair})} .$$

We expect, on average, x_E to be smaller for the direct production process (fig. 1(b)) than for the indirect one (parton scattering and subsequent fragmentation, fig. 1(a)). Thus we use the x_E dependence to investigate the contributions of the two processes.

The x_E distribution for the total sample is shown in fig. 3(b). It peaks at $x_E \simeq 0.5$. Hence we separate the events in two categories:

- Sample A: events with $0.5 < x_E < 1$.
- Sample B: events with $x_E \leq 0.5$.

The effective mass distributions for the high p_T pair of particles, interpreted as pions, are shown in figs 4(a,b) for samples A and B, respectively. The spectra were fitted with two relativistic Breit-Wigner functions BW(m) with masses and widths fixed at the Particle Data Group values [7] for the ρ^o and f^o mesons and a background parametrization

$$BG(m) \simeq (m - m_o)^{\alpha} \exp(\beta m + \gamma m^2) \qquad (2)$$

where m is the effective mass of the pair, m_o is set to 0.15 GeV and α, β, γ are the parameters in the fit. The fits take into account the reflections of the decays $K^{*o} \to K^+\pi^-$, $\bar{K}^{*o} \to K^-\pi^+$, $\phi \to K^+K^-$ into the $\pi^+\pi^-$

(*) The acceptance depends on the angular distribution of ρ^o decay. The decay distribution is expected to be isotropic for indirect ρ^o production while one expects a $\sin^2\theta$ distribution [2] (θ being the angle of the decay π^+ with respect to the ρ^o line-of-flight in the ρ^o restframe) in the case of direct production. In the extreme case of a pure $\sin^2\theta$ decay the cross section becomes $\sigma(\rho^o) = 0.58 \pm 0.2$ μb.

effective mass distribution, shown at the bottom of figs 4(a,b). The K^* and ϕ signals have been estimated both from the total sample and from the subsample in which one kaon was identified in the Cerenkovs.

The ρ^o signal N_ρ and the background BG are determined from the fit, by integrating respectively BW(m) and BG(m) in an interval of width Γ_ρ centred at the ρ^o mass. From these quantities we define $F_\rho = N_\rho/(N_\rho + BG)$.

The results of the fits are given in table 1. Good χ^2 values were obtained for both samples. We note a 38% increase in F_ρ in sample B over sample A: more ρ^o are produced, relative to background, in the region where direct production is favoured.

A number of checks were performed. For example the acceptance was evaluated for several extreme assumptions about the angular distributions of background and of ρ^o decays and this cannot explain the x_E dependence of F_ρ. In addition the X_E dependence persists when

- the sign of the opposite particle is chosen to be either positive or negative, or

- the samples are selected with $Y^{CM}_{pair} < 0$ (backward production of the ρ^o) or $Y^{CM}_{pair} > 0$ (forward production).

The experimental results are compared to two QCD models, using the Lund Monte-Carlo simulation and taking into account the experimental trigger conditions and the requirements (1).

(a) The standard Lund Monte-Carlo [8] which is based on leading order QCD parton scattering and subsequent fragmentation, yields the right order of magnitude for the inclusive cross section and reproduces satisfactorily the main features of the data, e.g. the shape of single particle spectra (not shown) and of the x_E and p_T distributions as shown in figs 3(b,c,d). The shape of the background is also well reproduced by the model in both x_E intervals. The amount of ρ^o production depends on a parameter of the model, the ratio α of vector meson/(vector + pseudoscalar meson) production in the fragmentation model. This parameter is not well determined; comparisons with data have given values in the range 0.25-0.60 [9]. In order to pursue the comparison with the model, the Monte-Carlo signal and background

have been normalized, summed over the two x_E regions, to the corresponding experimental values. In table 2(a) we give the expected numbers for ρ^o signal (N_ρ) and background (BG), now separately for the two x_E intervals. The x_E dependence of the background is well reproduced; however the model fails to predict the observed x_E dependence of N_ρ. A contingency table analysis [10] rules out the model predictions for N_ρ at a level below 0.1%. Attempts to reproduce the observed x_E dependence for N_ρ by modifications of other parameters of the model (e.g. the shape of the ρ^o fragmentation function) lead to inconsistencies [11] with other known data from deep inelastic lepton scattering [12].

(b) A modified Lund Monte-Carlo [13], where in addition to the leading order parton scattering diagrams, the contributions of the higher-twist processes:

quark + antiquark → gluon + ρ^o meson,

quark + gluon → quark + ρ^o meson

have been included.

These predictions come from new, detailed calculations of direct meson production [2]. The only adjustable parameter in establishing the direct cross sections is the exponent β which appears in the meson wave function $\phi \simeq f_\rho (x_q \cdot x_{\bar{q}})^\beta$ [2,14], where f_ρ is the ρ^o weak decay constant and x_q, $x_{\bar{q}}$ are the valence quark and antiquark momentum fractions in the ρ^o. However, this parameter β does not influence the x_E dependence of the direct ρ^o signal but only its intensity. To reproduce our data we have chosen $\beta = 1/4$; we note that for the pion form factor a value of $\beta = 1/4$ also appears to be favoured [14]. The results are shown in table 2(b); the x_E dependence of the ρ^o is now well reproduced as well as the background, which is the same as for model (a). We find that ~ 55% of the overall ρ^o signal, corresponding to a cross section of 0.30 ± 0.10 μb, comes from the higher twist contribution; the rest comes from fragmentation and corresponds to a value $\alpha = 0.3$. We note that this value is close to that obtained from recent e^+e^- data (TPC) [9] and from a detailed comparison [11] of the Lund model to deep inelastic lepton data. The lack of correlation between the x_E dependence of N_ρ and the charge of the opposite particle is also reproduced by the model. We note

that the model predicts a further enhancement of ρ^{o} production via higher twist mechanisms relative to fragmentation as the incident beam energy decreases. This will be tested in a future run of the experiment.

5. CONCLUSION

In summary, ρ^{o} production has been observed at high p_T in 300 GeV/c $\pi^{-}N$ interactions. The ρ^{o} fraction is $F_\rho = 0.21$ for the total sample. When separated into two categories in terms of the variable x_E an increase of 38% is observed in the ρ^{o} fraction F_ρ as x_E decreases. These observations are not compatible with leading order QCD only, which however reproduces the $\pi^{+}\pi^{-}$ background under the ρ^{o}. Good agreement is obtained when higher twist contributions are included. In the selected sample of events, they amount to about one half of the ρ^{o} signal and reproduce the observed dependence of F_ρ on x_E. We interpret this as evidence for direct ρ^{o} production via QCD higher twist processes.

Acknowledgements

We want to express our gratitude towards the members of the SPS, OMEGA, and Data Handling teams who contributed to several crucial stages in the preparation and running of the experiment.

REFERENCES

[1] E.L. Berger, T. Gottschalk and D. Sivers, Phys. Rev. D23 (1981) 99;
J.A. Bagger and J.F. Gunion, Phys. Rev. D25 (1982) 2287.

[2] M. Benayoun et al., CERN-TH 4368/86, to be published in Nuclear Physics.

[3] J. Badier et al., Zeitschr. für Phys. C11 (1981) 195;
M. Haguenauer et al., Phys. Lett. 100B (1981) 185;
D. Allasia et al., Phys. Lett. 124B (1983) 543;
J.J. Aubert et al., CERN/EP 85-72;
P.J. Fitch et al., CERN/EP 85-195;
C. Naudet et al., Phys. Rev. Lett. 56 (1986) 808;
S. Falciano et al., CERN/EP 86-35.

[4] W. Beusch, CERN/SPSC 77-70, SPSC/T17 (1977).

[5] W. Beusch et al., Nucl. Instr. and Meth. A249 (1986) 391.

[6] J.C. Lassalle, F. Carena and S. Pensotti, Nucl. Instr. & Meth. 176 (1980) 371.

[7] Review of Particle Properties, Rev. Mod. Phys., vol. 56, No. 2, part II, April 1984.

[8] H. Bengtsson and G. Ingelman, Computer Physics communication 34 (1985) 251;
T. Sjöstrand, Computer Physics communication 27 (1982) 243;
We have used the PYTHIA version 3.4 JETSET version 6.1;
B. Andersson, G. Gustafson, G. Ingelman and T. Sjöstrand, For a general review of the Lund model, Phys. Rep. 97, vol. 2 (1983) 31.

[9] R. Brandelik et al., (TASSO), Phys. Lett. 117B (1982) 135;
W. Bartel et al., (JADE), Phys. Lett. 145B (1985) 441;
H. Aihara et al., TPC/Two-GAMMA Collaboration, UCLA-85-015;
M. Derrick et al., (HRS) ANL-HEP-PR 85-20.

[10] See for instance: G.E.P. Box, W.G. Hunter and J.S. Hunter, Statistics for experiments, Wiley, New York, 1978.

[11] G. Ingelman, unpublished.

[12] K. Haacher, Thesis, WU B-DI 84-2 (1984);
J.J. Aubert et al., Phys. Lett. 133B, 5 (1983) 370.

[13] G. Ingelman et al., to be published.

[14] G.P. Lepage and S.J. Brodsky, Phys. Rev. D22 (1980) 2157.

TABLE 1

	N_ρ	BG	F_ρ	χ^2/NDF
$1 > x_E > 0.5$	3577 ± 190	16144 ± 200	0.181 ± 0.007	19/24
$x_E \leq 0.5$	4085 ± 160	12250 ± 180	0.250 ± 0.008	30/24

TABLE 2

- Errors on predictions reflect the Monte-Carlo statistics only.
- Monte-Carlo signal and background have been separately normalized, summed over the two x_E regions, to the corresponding experimental values.

	N_ρ	BG	F_ρ
(a) Lund model (leading order QCD)			
$1 > x_E > 0.5$	4310 ± 240	16149 ± 670	0.211 ± 0.014
$x_E \leq 0.5$	3352 ± 210	12245 ± 590	0.215 ± 0.016
(b) Modified Lund model (leading order + higher twist ρ_o)			
$1 > x_E > 0.5$	3686 ± 150	16149 ± 670	0.186 ± 0.010
$x_E \leq 0.5$	3976 ± 190	12245 ± 590	0.245 ± 0.015

FIGURE CAPTIONS

Fig. 1 (a) Example of a diagram for the indirect production of a ρ^{o} meson, in the reaction πN, via quark scattering and subsequent fragmentation.

(b) Example of a higher twist diagram for the direct production of a ρ^{o} meson.

(c) Transverse momentum selection to enhance a signal from the diagram of fig. 1(b).

Fig. 2 (a) Layout of the experiment.

(b) Perspective view of a reconstructed event showing three triggering tracks (π_1, π_2, π_3) with their hits in the hodoscopes (dot = slab hit). The "butterfly" shape of the hodoscopes prevents the recording of tracks with $p_T < 0.6$ GeV/c.

Fig. 3 (a) Mass spectrum for the pairs of oppositely charged high p_T particles.

(b) Distribution of $x_E = p_T(\text{opposite})/P_T(\text{pair})$ for the selected events.

(c) Distribution of $p_T(\text{pair})$.

(d) Distribution of $p_T(\text{opposite})$.

The dashed histograms are the results of a simulation using the Lund program [8] based on leading order QCD parton scattering and subsequent fragmentation.

Fig. 4 (a) As fig. 3(a) but for $0.5 < x_E < 1$. The results from the fit described in the text are indicated by: solid line: fitted mass spectrum, dashed line: fitted values of the function BG(m). The histograms at the bottom represents the reflection of the $\phi \to K^+K^-$ (dashed-dotted line) and $K^{*o} \to K^{\pm}\pi^{\mp}$ (dotted line) decay.

(b) As (a) but for $x_E \leq 0.5$.

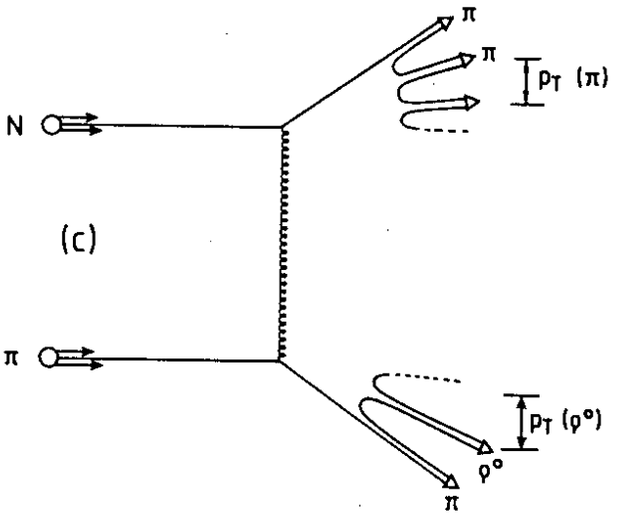
N
π
π
π
p_T (π)
(c)
π
p_T (ρ°)
ρ°
π

(a)

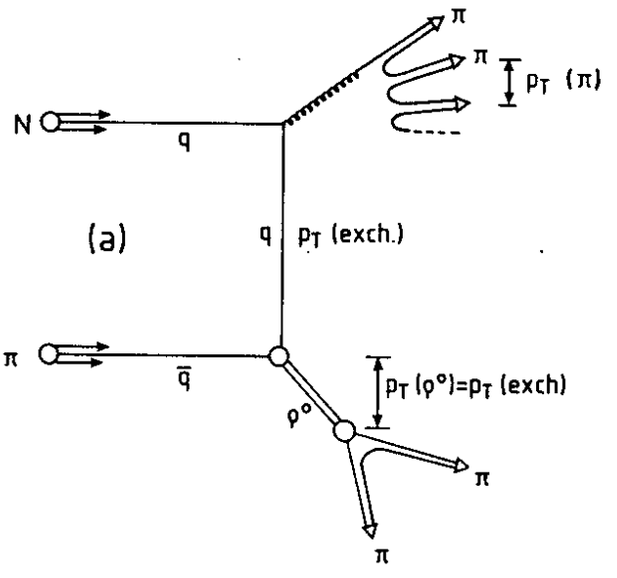
N
q
π
π
p_T (π)
(a)
q
p_T (exch.)
π
q̄
p_T (ρ°)=p_T (exch)
ρ°
π
π

(b)

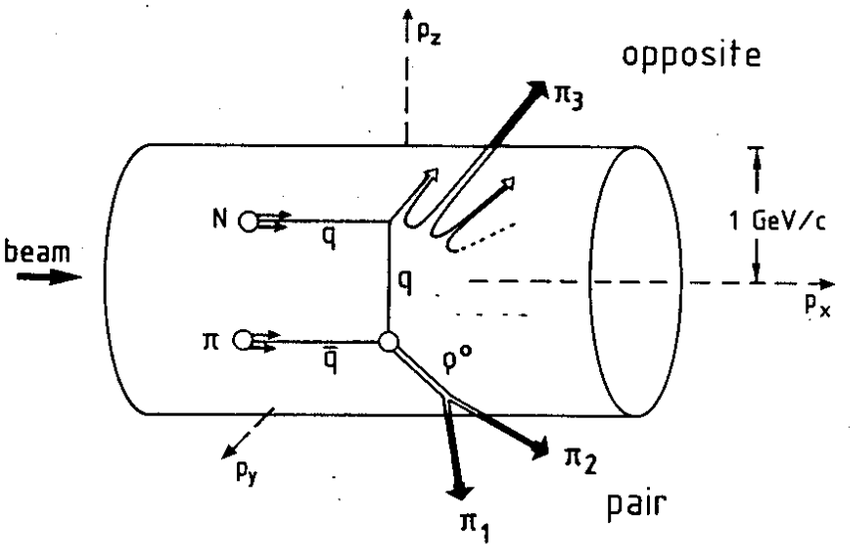
p_z
opposite
π_3
N
q
beam
q
1 GeV/c
p_x
π
q̄
ρ°
p_y
π_2
pair
π_1

(c)

Fig. 1

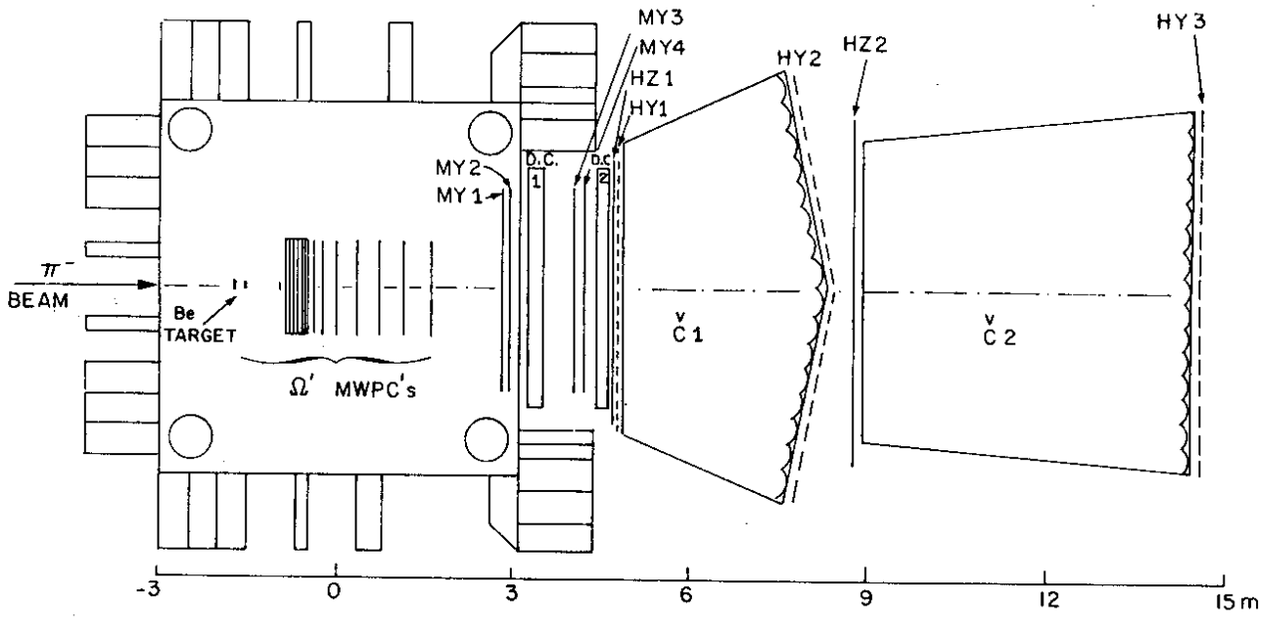
MY3
MY4
HZ1
HY1
HY2
HZ2
HY3
MY2
MY1
D.C. 1
D.C. 2
π⁻
BEAM
Be TARGET
Ω' MWPC's
ν C1
ν C2
-3
0
3
6
9
12
15m

(a)

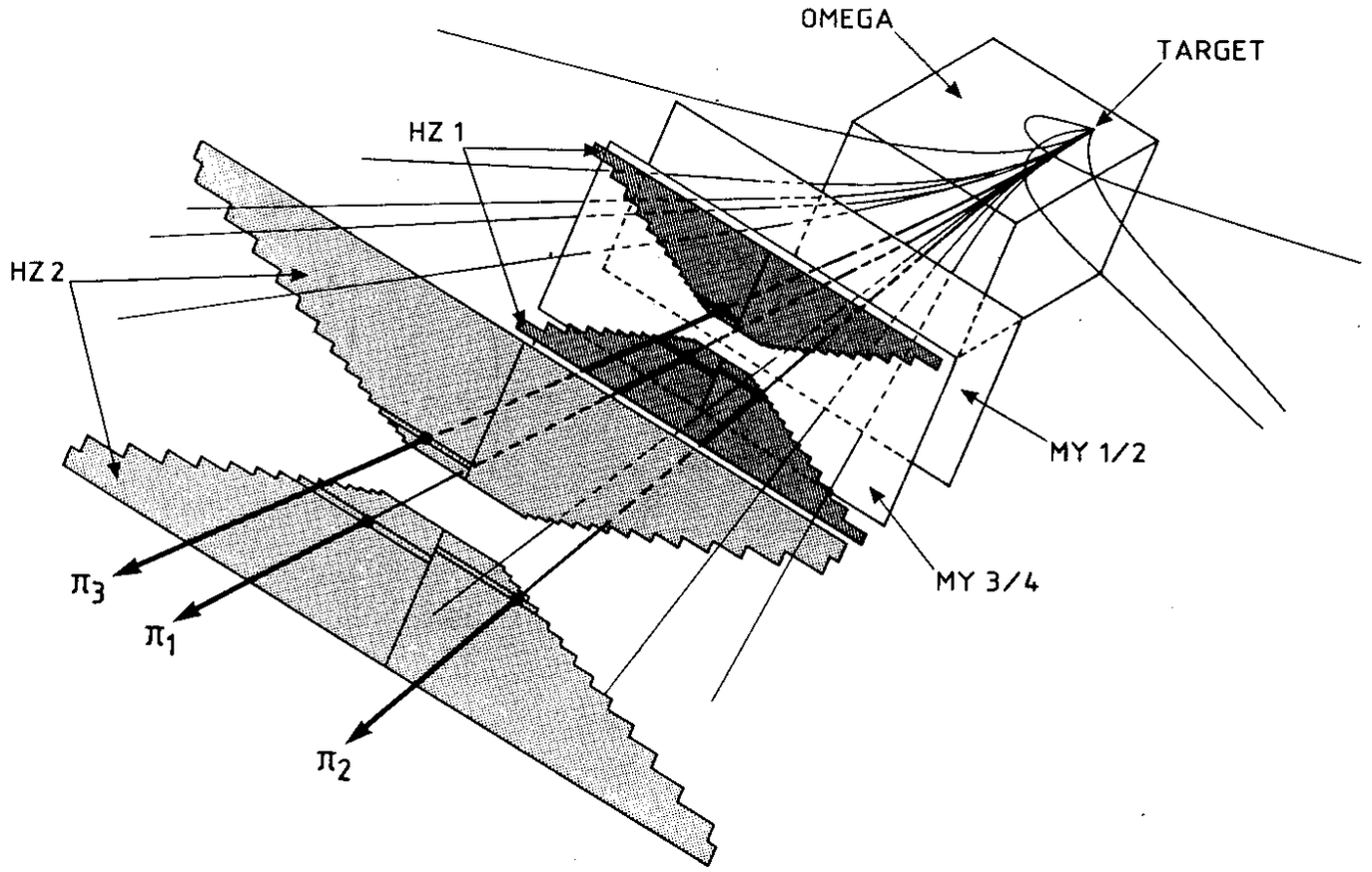
OMEGA
TARGET
HZ 1
HZ 2
MY 1/2
MY 3/4
π3
π1
π2

(b)

Fig. 2

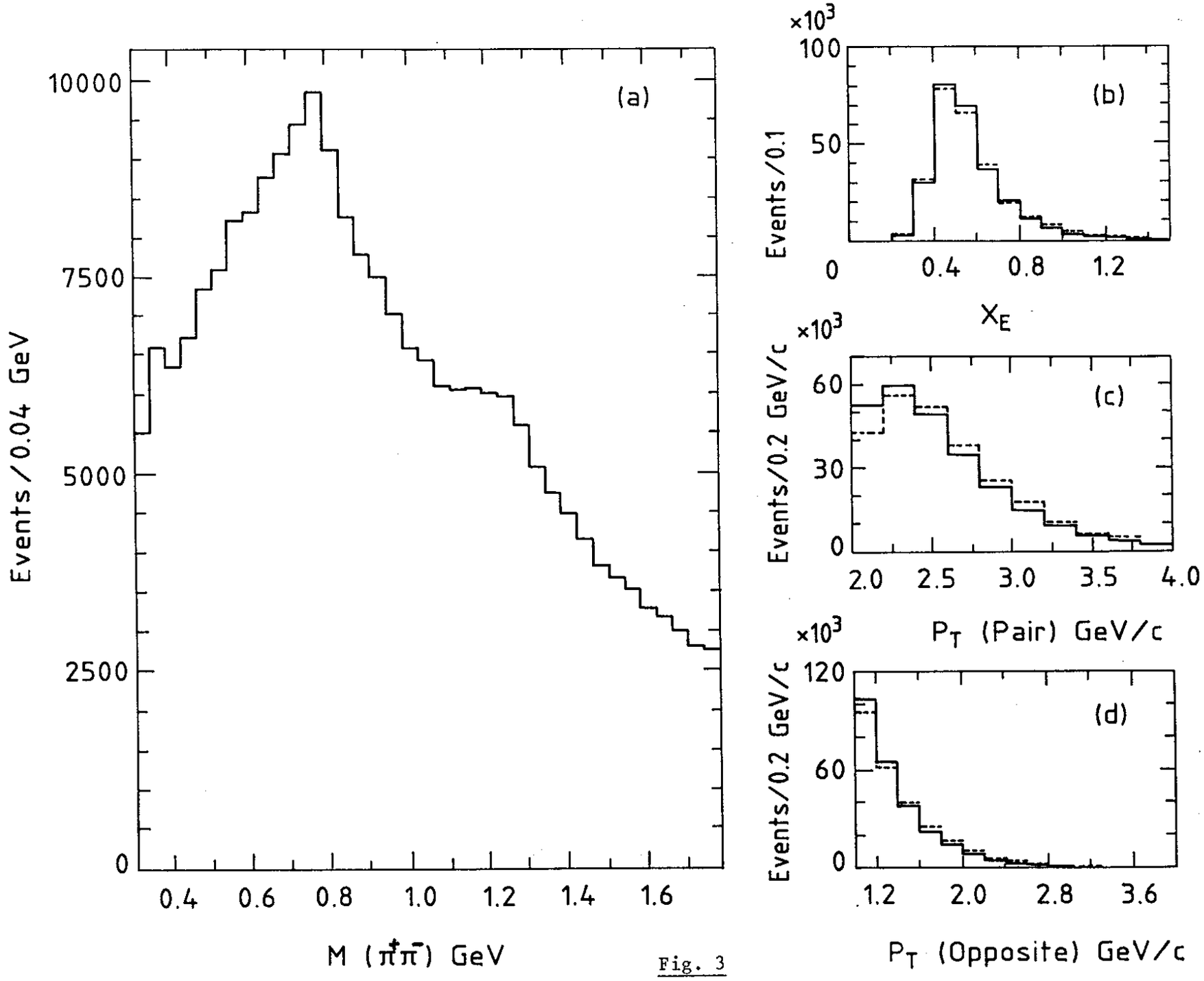
(a)
Events / 0.04 GeV
M ($\pi^+\pi^-$) GeV
(b)
Events / 0.1
X_E
(c)
Events/0.2 GeV/c
P_T (Pair) GeV/c
(d)
Events/0.2 GeV/c
P_T (Opposite) GeV/c

Fig. 3

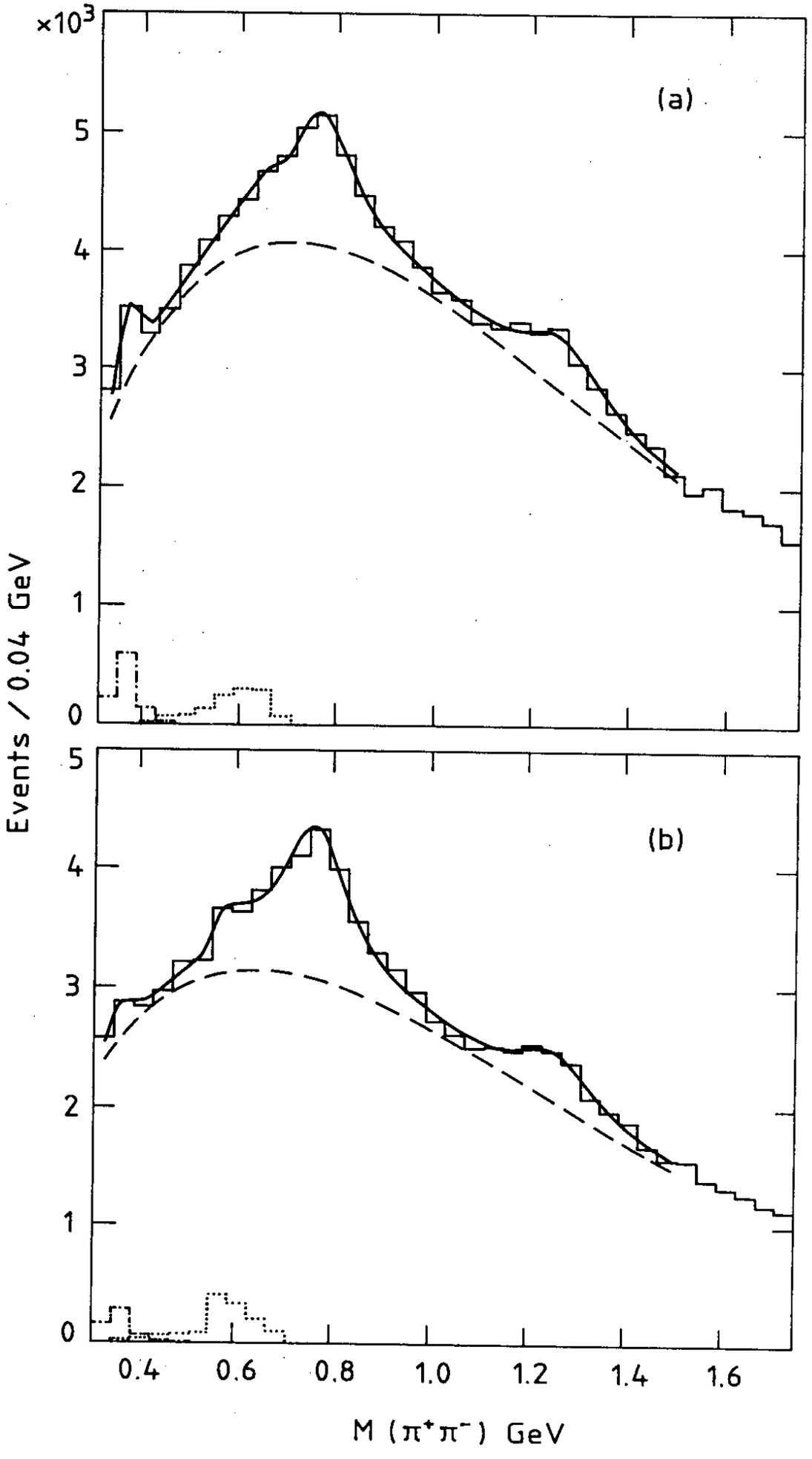

Fig. 4